Effect of Steps on the Decomposition of CH_3O at PdZn Alloy Surfaces

Zhao-Xu Chen,[†,‡] Kok Hwa Lim,[†] Konstantin M. Neyman,*[,§,||] and Notker Rösch*[,†]

Department Chemie, Technische Universität München, 85747 Garching, Germany, and Institució Catalana de Recerca i Estudis Avançats (ICREA), 08010 Barcelona, Spain

Received: November 10, 2004; In Final Form: January 4, 2005

The decomposition of methoxide (CH_3O) on a PdZn alloy is considered to be the rate-limiting step of steam re-forming of methanol over a Pd/ZnO catalyst. Our previous density functional (DF) studies (*Langmuir* **2004**, *20*, 8068; *Phys. Chem. Chem. Phys*. **2004**, *6*, 4499) revealed only a very low propensity of defect-free flat (111) and (100) PdZn surfaces to promote C−H or C−O bond breaking of CH_3O. Thus, we applied the same DF periodic slab-model approach to investigate these two routes of CH_3O decomposition on PdZn(221) surfaces that expose Pd, $(221)^{Pd}$, and Zn, $(221)^{Zn}$, steps. C−H bond cleavage of CH_3O is greatly facilitated on $(221)^{Pd}$: the calculated activation energy is dramatically reduced, to ∼50 kJ mol^{-1} from ∼90 kJ mol^{-1} on flat PdZn surfaces, increasing the rate constant by a factor of 10^8. The lower barrier is mainly due to a weaker interaction of the reactant CH_3O and an enhanced interaction of the product CH_2O with the substrate. The activation energy for C−O bond scission did not decrease on the $(221)^{Pd}$ step. On the $(221)^{Zn}$ step, the calculated reaction barriers of both decomposition routes are even higher than on flat surfaces, because of the stronger adsorption of CH_3O. Steps (and other defects) appear to be crucial for methanol steam re-forming on Pd/ZnO catalyst; the stepped surface $PdZn(221)^{Pd}$ is a realistic model for studying the reactivity of this catalyst.

1. Introduction

Catalytic steam re-forming of methanol is among the most attractive processes to produce in situ H_2 as an energy carrier alternative to conventional fuels.[1] Efficient catalysts based on a Pd/ZnO system have been proposed for steam re-forming.[2−4] The high performance of these catalysts was assigned to (1:1) PdZn alloy particles.[4−7] However, only very limited electronic and structural information on PdZn moieties at the atomic level has been available until very recently,[8,9] thus preventing detailed characterization of the active component of the catalyst and clarification of its function.

We have started systematic electronic structure investigations using density functional (DF) method to better understand the structure of Pd/ZnO catalysts[10−12] and their reactivity with respect to the initial phase of methanol steam re-forming.[13,14] This reaction is believed to begin with the formation of adsorbed methoxide, CH_3O, which decomposes further.[4] Therefore, our reactivity studies[13,14] focused on methoxide decomposition—as the probable rate-limiting step of the steam re-forming process—along two conceivable routes:[15−19] (i) C−H bond breaking, which leads to the formation of formaldehyde, CH_2O, and (ii) C−O bond scission, which results in adsorbed CH_3 species. As models of the active component of Pd/ZnO catalysts, we considered regular (defect-free) flat surfaces PdZn(111)[13] and PdZn(100);[14] these surfaces are likely exposed in (1:1) PdZn alloy.[10] Note that enrichment in Zn or Pd was calculated to be unfavorable on the (111) surface of the PdZn alloy;[11] lately, this computational finding was supported experimentally for the Pd/ZnO catalyst.[20] Our computational investigations based on DF studies of slab models[13,14] revealed that—on both PdZn(111) and PdZn(100) surfaces—the notably weaker C−H bond breaks much easier than the C−O bond. However, even the reaction channel of H-abstraction from CH_3O was predicted unlikely because of high activation barriers and unfavorable reaction energies.[13,14] Thus, active sites of Pd/ZnO catalysts that promote the decomposition of CH_3O are most likely located on defects, but not on planar surfaces.

This assumption is in line with the gradually growing evidence that defects play a central role in catalyzing various surface reactions. For instance, both experimental[21] and theoretical[22,23] studies show that reactions on metal catalysts are often completely dominated by steps. To examine whether defects also control the decomposition of CH_3O on Pd/ZnO catalysts, we performed theoretical studies of the C−H and C−O bond cleavage routes of this reaction on step sites of the PdZn(221) surface. To this end, we quantified and analyzed both thermodynamic and kinetic parameters that characterize these processes.

In section 2 of this paper we outline slab models employed for stepped PdZn(221) surfaces and we provide computational details. In section 3 we compare structures and energies of adsorption complexes relevant to C−H and C−O bond breaking of CH_3O with those on the flat (111) and (100) surfaces of PdZn. In section 4 we address calculated transition states (TS) and activation energies of CH_3O decomposition and discuss the feasibility of bond-breaking reactions on stepped surfaces. Finally, some conclusions are drawn.

2. Computational Details and Models

The PdZn(111) surface has been predicted to be exposed preferentially due to the lowest calculated surface energy.[10]

* Corresponding authors. E-mail addresses: (N.R.) roesch@ch.tum.de; (K.M.N.) konstantin.neyman@icrea.es.

[†] Technische Universität München.

[‡] Permanent address: Institute of Theoretical and Computational Chemistry, Department of Chemistry, Nanjing University, 210093, Nanjing, People's Republic of China.

[§] ICREA.

[||] Affiliated with Departament de Química Física i Centre especial de Recerca en Química Teòrica, Universitat de Barcelona i Parc Científic de Barcelona, 08028 Barcelona, Spain.

10.1021/jp044843e CCC: $30.25
Published on Web 02/22/2005

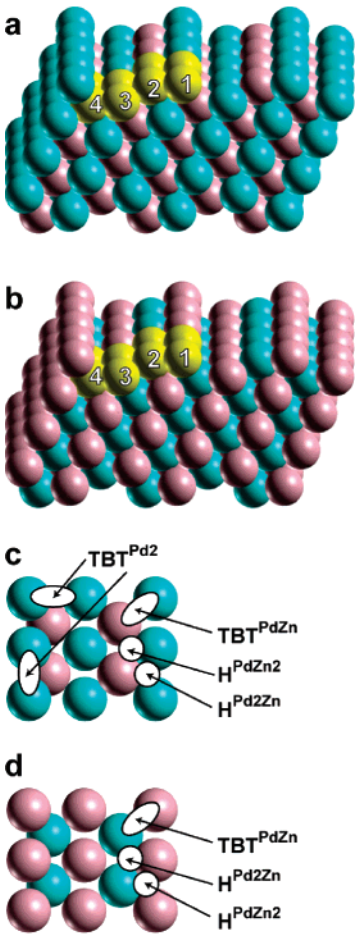

Figure 1. Slab models of PdZn(221) surfaces exposing (a) a step built of Pd atoms, $(221)^{Pd}$, (b) a step built of Zn atoms, $(221)^{Zn}$, and (c) and (d) selected adsorption sites on $(221)^{Pd}$ and $(221)^{Zn}$, respectively. Blue spheres, Pd; pink spheres, Zn. Yellow spheres indicate atoms in the surface unit cell; numbers identify the atomic rows at the terraces.

Thus, we selected the stepped surface PdZn(221) [4(111)×(111)] as model;[24] this surface features terraces of four atomic rows and a monatomic step, both of (111) orientation. We considered periodic slab models which consist of four stepped layers with eight atoms per layer in each unit cell (Figure 1). The slabs are separated by a vacuum spacing of ∼1.1 nm. There are two different types of stepped surfaces PdZn(221), depending on the atoms exposed by the steps: one, denoted $(221)^{Pd}$, exposes Pd steps and the other, $(221)^{Zn}$, features steps built of Zn atoms; we studied both types of models (Figure 1).

Stepped surfaces are assumed to undergo a notable relaxation with respect to bulk-terminated atomic positions.[24] Therefore, the top two stepped layers of PdZn(221) were relaxed (without an adsorbate), whereas the bottom two layers were kept frozen at the optimized truncated-bulk geometry.[10] This relaxation of the slab models lowered the total energy by 24 kJ mol^{-1} for $(221)^{Pd}$ and 26 kJ mol^{-1} for $(221)^{Zn}$. The substrate atoms were fixed at this relaxed geometry during the subsequent geometry optimization of adsorption complexes and the location of TS structures which were positioned on the relaxed side of the slab models; all degrees of freedom of the adsorbed moieties were optimized. We studied adsorption complexes of reactants and products involved in the decomposition of methoxide via C−H and C−O bond breaking: H, O, CH_3, CH_2O, and CH_3O.

According to our previous computational investigations on (111) and (100) surfaces of PdZn, H and C-bound CH_3 species prefer sites with mainly Pd atoms, while O and O-bound CH_3O species tend to occupy sites dominated by Zn atoms.[13,14] CH_2O molecules have been found to be very weakly bound to PdZn surfaces; they favor slightly a top-bridge-top configuration (TBT^{PdZn}), where C and O atoms of the adsorbate interact with substrate Pd and Zn atoms, respectively.[13] Therefore, on PdZn(221) surfaces, we only addressed adsorption complexes of H and CH_3 species at the sites T^{Pd} (top Pd) and H^{Pd_2Zn} (pseudo-hcp 3-fold hollow site, formed by one Zn and two Pd atoms in the upper slab layer), of O and CH_3O moieties on the sites T^{Zn} (top Zn) and H^{PdZn_2} (pseudo-hcp 3-fold hollow site of one Pd and two Zn atoms), and the TBT^{PdZn} structure of adsorbed CH_2O. Surface sites located directly at step edges or in their immediate vicinity are generally assumed to be more active than sites on terraces; therefore, only these former sites of PdZn(221) were considered when searching for preferred configurations of the adsorption complexes (see Figure 1 for pertinent adsorption sites).

The electronic structure calculations were performed with the projector-augmented plane-wave (PAW)[25,26] method as implemented in the code VASP[27−29] using the generalized-gradient exchange-correlation functional PW91.[30] For the integration over the Brillouin zone we combined (5 × 5 × 1) Monkhorst−Pack grids[31] with a generalized Gaussian smearing technique[32] (width, 0.15 eV). We adopted an energy cutoff of 400 eV throughout, which (according to our test calculations on adsorbed CO) enables convergence of adsorption energies to better than 1 kJ mol^{-1}.[13] Cartesian coordinates of the adsorbates were optimized until the force acting on each atom became less than 0.1 eV/nm. The binding energy (BE) of an adsorbate to the substrate,

$$\mathrm{BE} = E_{\mathrm{ad}} + E_{\mathrm{sub}} - E_{\mathrm{ad/sub}}$$

was calculated from the total energy $E_{ad/sub}$ of the slab covered with the adsorbate (in the optimized geometry) as well as from the total energies E_{ad} of the adsorbate in the gas phase and E_{sub} of the clean substrate. With this definition, a positive BE value corresponds to an exothermic adsorption process.

TS structures were located applying the nudged elastic band method[33] and verified by a vibrational analysis spectrum with one imaginary frequency. Reaction rate constants κ and preexponential factors A^0 for the decomposition of an adsorbate on a surface to two adsorbed fragments were calculated using transition-state theory:[34]

$$\kappa = \frac{k_B T}{h}\frac{q^*}{q} e^{-E_a/RT} = A^0 e^{-E_a/RT}$$

Here, k_B is the Boltzmann constant, h the Planck constant, E_a the activation energy corrected for zero-point vibrational energies, and R the gas constant. At a given temperature T (here adopted to be 300 K), the preexponential factor A^0 was determined by the partition functions q^* for the TS and q for the initial state (IS). The partition functions of adsorbed species contain neither translational nor rotational contributions, and the electronic contribution is unity as the electronic energy level splitting usually is ∼1 eV.[35] The remaining vibrational contributions were calculated in harmonic approximation.[35] Further computational details can be found elsewhere.[13,14]

3. H, O, CH_3, CH_2O, and CH_3O Species on PdZn(221) Surface: Adsorption and Energetics of CH_3O Decomposition Reactions

As already mentioned, the adsorbed species were studied on the relaxed PdZn(221) surface, which for convenience was represented by two slab models, $(221)^{Pd}$ and $(221)^{Zn}$, that merely

TABLE 1: Selected Interatomic Distances (A−B, pm)[a] and Binding (Adsorption) Energies (BE, kJ mol^{-1}) of Adsorbates Relevant to CH_3O Decomposition, Calculated on Favored Sites of PdZn(221) Surfaces Exposing Pd, $(221)^{Pd}$, and Zn, $(221)^{Zn}$, Steps[b]

		PdZn Surface			
adsorbate	param	$(221)^{Pd}$	$(221)^{Zn}$	$(111)^{c}$	$(100)^{d}$
H	H−Pd	176/176	184/184	183/183	190/190
	H−Zn		197	192	196
	BE	253	229	249	230
O	O−Pd	239	226	213	231
	O−Zn	191/191	189/189	193/193	198/198
	BE	407	472	449	458
CH_3	C−Pd	211	223	216	216
	BE	165	118	145	143
CH_2O	C−O	124	140	130	130
	O−Pd	293/230		271	283
	O−Zn	354	207/210	223	208
	C−Pd	317/371	219	225	227
	C−Zn	380			290
	BE	43	45	23	24
CH_3O[e]	O−Zn	304	203/203	211/211	219/224
	O−Pd	217/221	320/323	231	249/255
	C−O	145	144	143	145
	BE	204	262	221	234

[a] The two values *X*/*Y* listed for one pair of atoms A (of an adsorbate) and B (Pd or Zn of the substrate) indicate with which kind of hollow site, $PdZn_2$ or Pd_2Zn, atom A is interacting. [b] Also shown are adsorption parameters of the most stable complexes on the flat surfaces PdZn(111) and PdZn(100). [c] Reference 13. [d] Reference 14. [e] Another CH_3O adsorption complex, on the hollow site H^{PdZn_2} of the $(221)^{Pd}$ terrace, is equally stable, BE = 204 kJ mol^{-1}, as the complex on the step edge; its structural characteristics are O−Zn = 209/209 pm, O−Pd = 255 pm, and C−O = 143 pm.

differ by the two outermost stepped layers, exhibiting either Pd or Zn steps which were subject to relaxation. Before addressing structure and energetics of adsorption complexes, it is instructive to comment on the geometry of the relaxed $(221)^{Pd}$ and $(221)^{Zn}$ models. The PdZn(221) surface contains monatomic steps and four-atom wide (111) terraces composed of alternating rows of Pd and Zn atoms (Figure 1). The relaxation slightly shortens the heteronuclear bonds with respect to the calculated bulk-terminated values, at most by 10 pm for the distances between the less-coordinated edge atoms and their neighbors. Due to the smaller surface energy of Zn compared to Pd,[11] Zn atoms of a $(221)^{Pd}$ slab tend to move toward the surface, whereas Pd atoms move in the direction of the bulk; all calculated displacements were smaller than 16 pm. Homonuclear bond distances along the step (Figure 1) do not undergo any essential relaxation. However, homonulcear bond distances perpendicular to the step direction, i.e., bonds between the same type of atoms, one at a step edge and the other on the neighboring terrace, vary notably. Such nearest-neighbor bonds were calculated to shrink by 16 pm on $(221)^{Pd}$ and 11 pm on $(221)^{Zn}$ surfaces, while the corresponding next-nearest bond distances were extended by 13 and 5 pm, respectively; for details see Table 3S of the Supporting Information.

Table 1 shows selected distances and binding energy values for the five adsorbates under scrutiny, calculated at the most favorable sites on $(221)^{Pd}$ and $(221)^{Zn}$ surfaces of the PdZn alloy; for comparison, we also provide the results for the flat PdZn surfaces (111)[13] and (100).[14] In the following, we briefly discuss the data, emphasizing those differences brought by the presence of the Pd and Zn steps, which are reflected in altered reaction energies compared to the flat surfaces.

3.1. Hydrogen. On flat PdZn surfaces, H atoms prefer higher coordination sites dominated by Pd atoms.[13,14] On the $(221)^{Pd}$ surface, H was calculated to favor a bridge site on the step edge. The H−Pd distances are 7−14 pm shorter than on the flat surfaces, in line with the fact that adsorption energies are larger by 4−23 kJ mol^{-1} (Table 1); this can be rationalized by the enhanced bonding capability of edge Pd atoms due to their lower coordination. The preferred adsorption complex of H atom on the $(221)^{Zn}$ surface, on a 3-fold hollow Pd_2Zn site of the terrace, is destabilized by 24 kJ mol^{-1} compared to the most favorable complex on $(221)^{Pd}$; it features somewhat longer H−Pd distances.

3.2. Oxygen. The most stable position of adsorbed O on a $(221)^{Pd}$ surface is a hollow site formed by an edge Pd atom and two Zn atoms of the second row (see Figure 1). There, despite slightly shorter O−Zn bond lengths, the interaction with the substrate is notably reduced, by 40−50 kJ mol^{-1}, with respect to the flat surfaces (Table 1). On the $(221)^{Zn}$ surface, atom O preferentially occupies a 3-fold hollow site comprising two edge Zn atoms and one Pd atom of the second row (Figure 1). This moiety is most strongly bound among all PdZn adsorption complexes considered so far, 65 kJ mol^{-1} stronger than on $(221)^{Pd}$ and ∼10−20 kJ mol^{-1} stronger than on the flat surfaces.

3.3. Methyl. While H atoms favor hollow sites, CH_3 adsorbates favor sites on top of Pd.[13,14] At the $(221)^{Pd}$ surface, CH_3 prefers to be located on top of a step-edge Pd atom. There is an energy gain of ∼20 kJ mol^{-1} with respect to adsorption on the (111) and (100) surfaces, accompanied by a reduced C−Pd bond length (Table 1). The interaction of CH_3 with the $(221)^{Zn}$ model was calculated to be the weakest among all methyl adsorption complexes studied so far (∼25 kJ mol^{-1} less than on the flat surfaces[13,14]), and it features the longest C−Pd bond.

3.4. Formaldehyde. The adsorption of CH_2O on flat PdZn surfaces was calculated to be very weak, less than 25 kJ mol^{-1}.[13,14] On both surfaces, $(221)^{Pd}$ and $(221)^{Zn}$, the adsorption energies are increased by ∼20 kJ mol^{-1} (Table 1) to values comparable to the interaction on the Pd(111) surface,[13] but the binding energies on PdZn(221) are still rather small. The adsorption complex of CH_2O on $(221)^{Pd}$ has a pseudo-top-bridge-top structure (TBT^{Pd_2}; see Figure 1) with the O atom over a step Pd atom and the C atom on top of a Pd atom at the lower terrace. On $(221)^{Zn}$, the O atom binds to two step Zn atoms with almost equal bond lengths, and the C atom attaches to a Pd atom of the upper terrace. The C−O bond is essentially in the symmetry plane that is normal to the step edge. Also, due to the shallow potential energy surfaces, structural details of the adsorption complexes of CH_2O appear to be less significant in the context of the present study (see Table 1 and Table 4S of the Supporting Information).

3.5. Methoxide. On the $(221)^{Pd}$ surface, CH_3O is calculated to adsorb in a bridge position, bound to two edge Pd atoms with relatively short O−Pd distances of 217 and 221 pm; the nearest O−Zn contact of 304 pm is essentially nonbonding. The C−O bond of 145 pm is tilted 40° from the perpendicular of the (111) terraces. The calculated adsorption energy of 204 kJ mol^{-1}—the lowest one among the methoxide complexes presently discussed (Table 1) —reflects the fact that favorable O−Zn interactions are absent in this structure. The C−O stretching frequency is shifted down to 925 cm^{-1} compared to 1114 cm^{-1}, calculated for gas-phase CH_3O. With BE = 204 kJ mol^{-1} (see footnote *e* to Table 1), methoxide species adsorbed on the hollow sites H^{PdZn_2} of $(221)^{Pd}$ terraces are as stable as the structure on the step edges just discussed. The most favorable adsorption site of CH_3O on PdZn studied so far is at a step-bridge site of the $(221)^{Zn}$ surface (Table 1); the calculated

TABLE 2: Thermodynamic and Kinetic Parameters Calculated for C−H and C−O Bond Breaking of CH_3O on Stepped PdZn(221) Surfaces in Comparison with the Analogous Reactions on the Flat Surfaces PdZn(111) and PdZn(100)[a]

		sites on PdZn				
param		$(221)^{Pd}$ terrace	$(221)^{Pd}$ edge	$(221)^{Zn}$	$(111)^b$	$(100)^c$
C−H	E_r[d]	17	17	97	61	89
	E_a	49	53	108	93	90
	A^0	3×10^{13}	2×10^{13}	6×10^{12}	1×10^{13}	2×10^{12}
	κ	7×10^{4}	1×10^{4}	1×10^{-6}	8×10^{-4}	4×10^{-4}
C−O	E_r[d]		65	105	60	65
	E_a		199	220	198	158
	A^0		8×10^{12}	4×10^{12}	1×10^{12}	2×10^{12}
	κ		$\sim 10^{-22}$	$\sim 10^{-26}$	$\sim 10^{-22}$	$\sim 10^{-15}$

[a] Heats of reaction E_r (kJ mol^{-1}), activation energies E_a (kJ mol^{-1}) corrected for vibrational zero-point energies, preexponential factors A^0 (s^{-1}), and reaction rate constants κ (s^{-1}) at 300 K. [b] Reference 13. [c] Reference 14. [d] The heat of reaction is calculated as $E_r = \Sigma E_P - \Sigma E_R - \Sigma BE_P + \Sigma BE_R$, where ΣE_P and ΣE_R are sums of the total energies E of products (P) and reactants (R), respectively, in the gas phase. ΣBE_P and ΣBE_R are sums of the (adsorbate−substrate) binding energies BE of isolated product and reactant species, respectively. A positive value of E_r characterizes an endothermic reaction.

binding energy of 262 kJ mol^{-1} is 41 and 28 kJ mol^{-1} more stable than the preferred sites on (111) and (100) surfaces, respectively. The complex $CH_3O/PdZn(221)^{Zn}$ exhibits the shortest CH_3O−Zn bond overall and a C−O vibration at 993 cm^{-1}.

The above comparison of adsorption geometries and energies on the stepped and flat PdZn surfaces does not exhibit particularly large changes (Table 1). However, there is a clear trend that the Pd and Zn atoms located at steps form somewhat stronger bonds with all adsorbates under discussion than sites of flat PdZn surfaces; obviously due to their lower coordination numbers, atoms at step sites feature a higher unsaturated valence than atoms on terraces. The binding energies on flat surfaces are between those on the two stepped surfaces, $(221)^{Pd}$ and $(221)^{Zn}$ (Table 1).

Finally we discuss the consequences of these bond strengthening effects for adsorbed CH_3O reactants in the IS as well as for the products in the final state (FS) of either bond breaking reaction, $CH_2O + H$ (C−H) and $CH_3 + O$ (C−O). The overall changes for stepped PdZn surfaces result in a more or less favorable reaction energetics (heat of reaction), compared to flat PdZn surfaces. Recall that on flat PdZn surfaces both the C−H and C−O decomposition channels were calculated to be endothermic, with heats of reaction of 61 and 89 kJ mol^{-1} (C−H) and 60 and 65 kJ mol^{-1} (C−O) on PdZn(111)[13] and PdZn(100),[14] respectively. On the basis of the calculated reaction energies for stepped substrate models, C−H bond scission on $(221)^{Pd}$ is ~40 kJ mol^{-1} *less endothermic* than on PdZn(111) and ~70 kJ mol^{-1} less endothermic than on PdZn(100). On the other hand, C−H bond breaking reaction on the $(221)^{Zn}$ surface is *more endothermic* than on the flat surfaces, ~40 kJ mol^{-1} on (111) and ~10 kJ mol^{-1} on (100). Neither $(221)^{Pd}$ nor $(221)^{Zn}$ step sites help to render C−O bond breaking thermodynamically more favorable (i.e., less endothermic) than on the flat (111) and (100) surfaces. In summary, of the step surface sites of PdZn(221) considered here, only the $(221)^{Pd}$ surface appears to offer favorable thermodynamics for C−H bond breaking of CH_3O; for a more detailed account of the calculated heats of reaction, see Table 2.

4. Kinetics of CH_3O Decomposition on PdZn(221) Surface

As already mentioned, there are two local minima for CH_3O adsorbates on the stepped $(221)^{Pd}$ surface which feature the same stability: at step-edge bridge sites and at hollow sites on terraces. As step sites are considered to be more active than sites of terraces,[21] we chose the former structure to model the IS of methoxide decomposition on this surface (Figures 2a,b and 3).

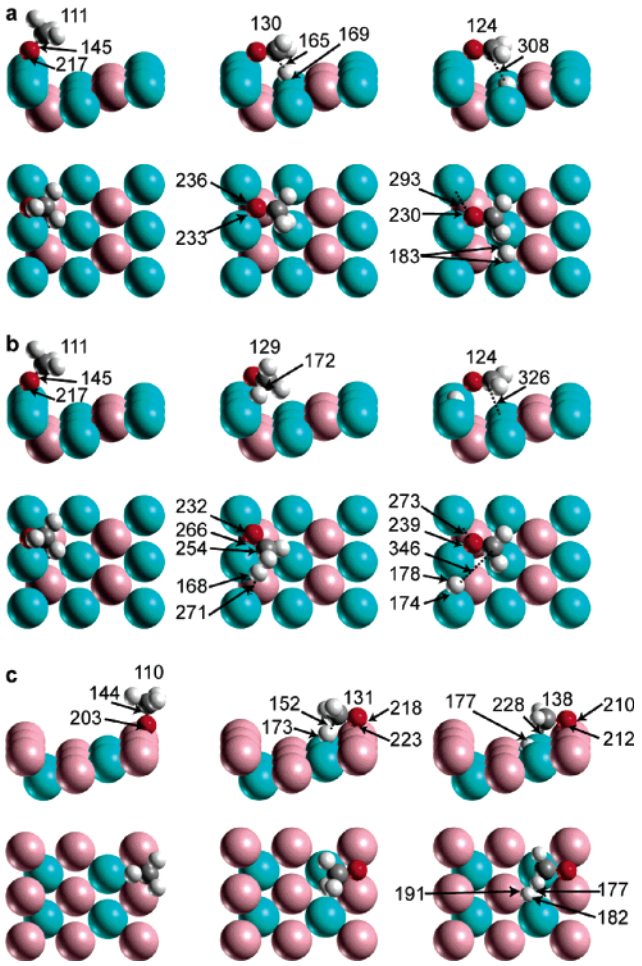

Figure 2. Side (upper panels) and top views (lower panels) of calculated IS, TS, and FS structures involved in three routes of C−H bond breaking of CH_3O on PdZn(221) surfaces: (a) dissociated H on the $(221)^{Pd}$ terrace, (b) dissociated H on the $(221)^{Pd}$ step, and (c) on $(221)^{Zn}$. Selected bond lengths are given in picometers. Atomic spheres: blue, Pd; pink, Zn; red, O; dark gray, C; light gray, H.

The choice of the IS structure on the $(221)^{Zn}$ surface is unequivocal (see above and Figure 2c).

4.1. C−H Bond Cleavage. On the $(221)^{Pd}$ surface, we located two TS structures for C−H bond cleavage that differ in the position of the dissociated hydrogen atom (H_a). In the first structure (referred to as TS^{terr}), H_a ends up on a terrace site, whereas in the second structure (referred to as TS^{edge}), H_a is finally positioned on a bridge site at the Pd step edge. The TS

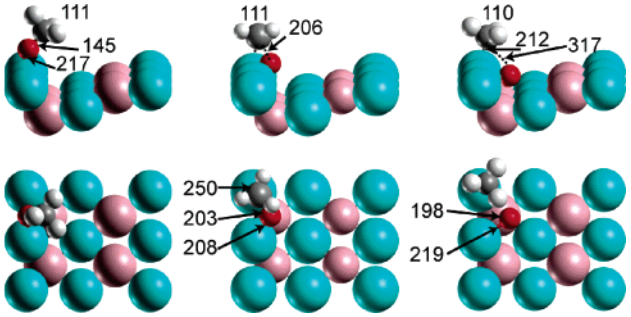

Figure 3. Side (upper panels) and top views (lower panels) of calculated IS, TS, and FS structures involved in the lowest barrier route of C−O bond breaking of CH_3O on the PdZn surface $(221)^{Pd}$.

of C−H cleavage on the $(221)^{Zn}$ surface is characterized by a bridge position of the atom O on the Zn step edge. In the following, we will briefly describe the profiles of C−H bond breaking of CH_3O and we will characterize the TS structures (Figure 2a−c). The corresponding calculated kinetic parameters are collected in Table 2.

TS with H_a on the Terrace of $(221)^{Pd}$. The reaction via TS^{terr} to FS (Figure 2a), in which H_a is located on a terrace, begins with the C−O bond tilting of CH_3O toward the terrace. After sufficient progress, this motion eventually allows a H_a−Pd interaction with a concomitant weakening of the C−H_a bonding. In the TS^{terr}, the nearest H_a−Pd contact reaches 169 pm, whereas the C−H_a length increases from 111 to 165 pm. These distances are somewhat shorter than on a flat (111) surface, H_a−Pd = 177 pm and C−H_a = 170 pm.[13] In the TS, the C−O bond, 130 pm, is almost perpendicular to the step orientation. The O atom is basically at a step-edge bridge site, with two O−Pd distances of 233 and 236 pm. In the FS, the atom H_a sits on the bridge site exactly between two terrace Pd atoms at distances of 183 pm. The calculated zero-energy corrected activation barrier for this reaction path, 49 kJ mol^{-1}, is more than 40 kJ mol^{-1} *lower* than the corresponding barriers on the (111) and (100) surfaces. As a consequence, the reaction rate constant at 300 K, 7×10^4 s^{-1}, is 10^8 times larger than on the flat surfaces (Table 2). Such a significant rate constant indicates that C−H bond breaking of adsorbed methoxide on the stepped $(221)^{Pd}$ surface is feasible with a high yield, at variance with the very low activity of terrace sites studied previously.

TS with H_a on the Step Edge of $(221)^{Pd}$. Similarly to the above reaction, this path (via TS^{edge}) also starts with tilting of the C−O bond but in a different direction—almost parallel to the step. In the TS^{edge}, the C−O axis forms an angle of ∼60° with the step (Figure 2b). The O atom is in a distorted edge-bridge position with O−Pd contacts of 232 and 266 pm. The C−O bond in TS^{edge} is almost as long as for the former path and in the TS on the PdZn(111) surface.[13] The H_a atom is displaced toward an edge-bridge site; H_a−Pd distances are 168 and 271 pm. The C−H_a bond in TS^{edge}, 172 pm, is 7 pm longer than that in TS^{terr}. After the TS^{edge} has been reached, the C−O bond re-directs to the lower terrace. In the FS, the C−O axis is almost perpendicular to the step edge (Figure 2b) and the O−Pd distances are stretched to 239 and 273 pm. H_a moves to the edge-bridge site and forms nearly equal H_a−Pd contacts of 178 and 174 pm. The calculated activation barrier for this path, 53 kJ mol^{-1} (Table 2), is again much lower than the barriers calculated on flat PdZn surfaces, and it is only slightly higher than the barrier for the profile via TS^{terr}. Concomitantly, the rate constant at 300 K, $\sim 10^4$ s^{-1}, is only several times smaller than for the first path, but dramatically higher than on the flat planes (Table 2). The reasons for lowering the activation barrier for C−H bond breaking on the $(221)^{Pd}$ surface compared to the flat surfaces will be discussed in subsection 4.3.

TS on $(221)^{Zn}$. Not unexpectedly, the C−H bond-breaking reaction on the $(221)^{Zn}$ surface at a Zn bridge (Figure 2c) features C−O bond tilting toward a terrace Pd atom. As this is a (111) terrace, the reaction proceeds similarly to that on the PdZn(111) surface,[13] except that the oxygen center, instead of moving to a top Zn location, remains essentially at the Zn bridge site due to the strong O−Zn interaction here. Along the reaction path, the distance H_a−Pd decreases, manifesting a bonding interaction of these two atoms. In the TS, the activated C−H_a bond is stretched to 152 pm and the H_a−Pd contact is 173 pm; the O−Zn distances are 218 and 223 pm. In the FS, H_a moves to the Pd_2Zn site with H_a−Pd distances at 177 and 182 pm and the H_a−Zn distance at 191 pm, while the O−Zn bonds are 210 and 212 pm. The present reaction profile is characterized by a large barrier of 108 kJ mol^{-1}, resulting in a negligible reaction rate (Table 2). The main reason for the relatively high barrier on $(221)^{Zn}$ is the enhanced interaction of the reactant CH_3O with the substrate. Therefore, this reaction route is not expected to play a role in the overall reaction mechanism of methoxide decomposition.

4.2. C−O Bond Cleavage. To reiterate, on flat PdZn surfaces methoxide decomposition via C−O bond cleavage was calculated notably less favorable than C−H bond breaking.[13,14] As shown in section 3, the C−O bond-breaking process on PdZn-(221) sites is even further disfavored thermodynamically with respect to the corresponding reaction on the planar (111) and (100) surfaces (Table 2). To examine whether the presence of steps on PdZn catalysts facilitates kinetically the breaking of the C−O bond, we located three TS structures on the $(221)^{Pd}$ surface and one on $(221)^{Zn}$ and we quantified the activation barriers (see Tables 6S and 7S of the Supporting Information).

TS with CH_3 on Step Edge of $(221)^{Pd}$. In the TS^{edge}, the leaving O atom is approaching a Zn atom below the Pd step. Tilting the C−O bond starts the reaction. Eventually the CH_3 group moves toward the top site on a step-edge Pd while the O atom is displaced to a Zn atom at the bottom of the step (Figure 3). Compared to that in the IS, the O−Zn contact is shortened by 75 pm in the TS^{edge}, whereas the C−O distance is stretched by ∼60 to 206 pm, almost equal to that calculated on the (111) surface.[13] In the FS^{edge}, the O atom reaches the hollow site formed by one bottom Zn atom and two edge Pd atoms; see selected distances in Figure 3. The calculated activation energy, 199 kJ mol^{-1}, is the lowest one found in the present study for this reaction path (Table 2). The barrier is almost equal to that on the (111) surface which yielded a very low rate constant and similar structural motifs of the transformation. Recall that the corresponding barrier on the (100) surface is ∼40 kJ mol^{-1} lower. C−O bond breaking was calculated somewhat more endothermic because the bonding of O to the $(221)^{Pd}$ substrate is weaker than on the (111) and (100) surfaces (Table 1).

Other Reaction Profiles of C−O Bond Breaking. The profiles of all other C−O bond-breaking reactions studied in this work, i.e., for the substrate PdZn(221) with Pd and Zn steps, are characterized by even higher activation energies of 207 and 273 kJ mol^{-1} for C−O breaking on $(221)^{Pd}$, and 220 kJ mol^{-1} for C−O cleavage on $(221)^{Zn}$ (see Tables 6S and 7S of the Supporting Information). Therefore, details of the corresponding IS, TS, and FS structures would only be interesting if one wants to analyze which interactions contribute to the increase of the barrier. However, this issue has already been covered when comparing the results obtained for C−O bond breaking on the (111) and (100) surfaces of PdZn.[13,14]

4.3. Analysis of the Barrier Height Alterations Compared to PdZn(111) Surface. The calculated activation energies for C−H bond splitting of methoxide on the (111) and (100) surfaces of PdZn[13,14] are rather close to each other and reflect the low reactivity of these substrates (Table 2). In view of this similarity, we have chosen the (111) surface as reference for our attempt to rationalize why the activation energy for C−H scission on the $(221)^{Pd}$ surface is more than 40 kJ mol^{-1} smaller than on the reference (111) while the activation energy of C−O scission is not lowered.

In general, the activation barrier of a reaction over various kinds of substrates may change because the (total) energies of the reactant(s) or the TS complex vary. In case of a decomposition reaction AB → A + B, the second contribution can be approximated in terms of the interaction energies of the product species A and B with the substrate, taken in the geometry of the TS complex. A similar TS analysis has been performed for instance in ref. 36. In the following we will explore this situation in more detail.

Relative to the activation energy calculated for PdZn(111), the reaction barrier of C−H scission on $(221)^{Pd}$ is 44 kJ mol^{-1} lower via TS^{terr} and 40 kJ mol^{-1} lower via TS^{edge} (Table 2). As measured by the adsorption energy, on the $(221)^{Pd}$ surface of PdZn, the energy of the reactant CH_3O is raised 17 kJ mol^{-1} above the energy on the PdZn(111) surface (Table 1). In other words, the activation energy is lowered by 17 kJ mol^{-1} because the reactant interacts weaker with the $(221)^{Pd}$ surface than with the (111) surface. The product fragment CH_2O, fixed in the TS^{terr} and TS^{edge} geometries, interacts 32 and 51 kJ mol^{-1} more strongly with the substrate than in the structure of the (111) TS on that substrate. The corresponding values for H species imply weaker interaction energies by 8 and 15 kJ mol^{-1}. Accordingly, one expects a total lowering of the activation barrier by 24 kJ mol^{-1} (TS^{terr}) or 36 kJ mol^{-1} (TS^{edge}) due to the changes in the interactions of the products CH_2O and H with the substrate. In the gas phase, the TS fragments, fixed in their TS structure of the corresponding adsorption complex, interact 7 kJ mol^{-1} stronger (TS^{terr}) and 9 kJ mol^{-1} weaker (TS^{edge}) than in the (111) TS. Together with the absorbate−substrate interaction and the IS contribution of 17 kJ mol^{-1}, one estimates a total lowering of the barrier height on $(221)^{Pd}$ over that on the (111) surface by 48 kJ mol^{-1} (TS^{terr}) or 44 kJ mol^{-1} (TS^{edge}). These approximate values are not far from the results calculated for TS^{terr}, 44 mol^{-1}, and TS^{edge}, 40 mol^{-1} (Table 2). Phrased differently, the enhanced (total) stabilization of the products contributes about twice as much to the lowering of the activation barrier than the weaker interaction of the reactants.

A similar analysis of C−O bond scission on the $(221)^{Pd}$ surface in comparison with the barrier on the surface PdZn-(111) assigns the largest unfavorable contribution to the O atom, e.g., −78 kJ mol^{-1} in TS^{edge}. This change reflects the weaker O-substrate interaction at $(221)^{Pd}$ surface compared to (111). In TS^{edge}, the other product species, CH_3, contributes 18 kJ mol^{-1} to a lower relative barrier height, so that the combined product effect is an *increase* of the $(221)^{Pd}$ barrier relative to that of the (111) substrate by (78 − 18) kJ mol^{-1} = 60 kJ mol^{-1}. The gas-phase correction of this estimate is very small: the TS^{edge} structure is 1 kJ mol^{-1} higher in energy than the (111) TS. In combination with the favorable initial state effect, 17 kJ mol^{-1} (see above), and absorbate−substrate interaction, one estimates the activation barrier on $(221)^{Pd}$ to be 44 kJ mol^{-1} higher than on PdZn(111). The discrepancy between estimated and calculated change of the barrier height may be traced back to bond competition.[37] Indeed, the bond distance of O in TS^{edge} to the shared Pd atom, 203 pm (Figure 3), is notably shorter than the value 238 pm calculated for the TS on (111).[13]

5. Conclusions

In this paper we performed slab-model DF investigations on the decomposition of methoxide at PdZn(221) surfaces featuring Pd or Zn steps. The most favorable adsorption complexes involve step-edge atoms, consistent with the higher reactivity of low-coordinated atoms forming a step. The binding energies on stepped $(221)^{Pd}$ and $(221)^{Zn}$ substrate models exhibit an obvious trend: species preferring Pd-dominated sites feature the strongest binding on $(221)^{Pd}$, while for adsorbates favoring Zn-dominated sites the adsorption interaction is the strongest on the $(221)^{Zn}$ slab.

Compared to the flat PdZn surfaces studied previously, the activation energies for C−H and C−O bond cleavage on the $(221)^{Zn}$ surface do not decrease, even though methoxide interacts stronger with the substrate at the Zn step edge. On the other hand, the reaction barrier for C−H bond breaking on the $(221)^{Pd}$ surface is greatly reduced to ∼50 kJ mol^{-1} from ∼90 kJ mol^{-1} on flat surfaces. This crucial activation barrier is reduced for two synergetic reasons: the reactant CH_3O interacts weaker with the catalyst while the product CH_2O binds stronger to the substrate. Concomitantly, the calculated reaction rate constant for C−H cleavage is increased by a factor of 10^8, reaching $\sim 10^4-10^5$ s^{-1} at 300 K. Such large rate constants qualify the present model for C−H bond breaking of CH_3O adsorbed on PdZn surfaces as realistic. Thus, one expects this reaction is completely dominated by step sites and/ or other defects.

Acknowledgment. K.H.L. gratefully acknowledges a fellowship of Deutscher Akademischer Austauschdienst (DAAD). This work was supported by Deutsche Forschungsgemeinschaft and Fonds der Chemischen Industrie (Germany).

Supporting Information Available: Cartesian coordinates of bulk-terminated PdZn(221) slab models, of the corresponding relaxed slab models, and of all pertinent adsorption complexes and transition states and corresponding total PW energies as well as the vibrational modes of pertinent molecular adsorption complexes and transition states are also given. This material is available free of charge via the Internet at http://pubs.acs.org.

References and Notes

(1) Ogden, J. M. *Annu. Rev. Energy Environ.* **1999**, *24*, 227.
(2) Trimm, D. L.; Önsan, Z. I. *Catal. Rev.−Sci. Eng.* **2001**, *43*, 31.
(3) Iwasa, N.; Kudo, S.; Takahshi, H.; Masuda, S.; Takezawa, N. *Catal. Lett.* **1993**, *19*, 211.
(4) Iwasa, N.; Takezawa, N. *Top. Catal.* **2003**, *22*, 215.
(5) Takezawa, N.; Iwasa, N. *Catal. Today* **1997**, *36*, 45.
(6) Cubeiro, M. L.; Fierro, J. L. G. *J. Catal.* **1998**, *179*, 150.
(7) Pfeifer, P.; Schubert, K.; Liauw, M. A.; Emig, G. *Appl. Catal., A* **2004**, *270*, 165.
(8) Rodriguez, J. A. *J. Phys. Chem.* **1994**, *98*, 5758.
(9) Rodriguez, J. A.; Kuhn, M. *J. Phys. Chem.* **1996**, *100*, 381.
(10) Chen, Z.-X.; Neyman, K. M.; Gordienko, A. B.; Rösch, N. *Phys. Rev. B: Condens. Matter Mater. Phys.* **2003**, *68*, 07514.
(11) Chen, Z.-X.; Neyman, K. M.; Rösch, N. *Surf. Sci.* **2004**, *548*, 291.
(12) Neyman, K. M.; Sahnoun, R.; Inntam, C.; Hengrasmee, S.; Rösch, N. *J. Phys. Chem. B* **2004**, *108*, 5424.
(13) Chen, Z.-X.; Neyman, K. M.; Lim, K. H.; Rösch, N. *Langmuir* **2004**, *20*, 8068.
(14) Chen, Z.-X.; Lim, K. H.; Neyman, K. M.; Rösch, N. *Phys. Chem. Chem. Phys.* **2004**, *6*, 4499.
(15) Chen, J.-J.; Jiang, Z.-C.; Zhou, Y.; Chakraborty, B. R.; Winograd, N. *Surf. Sci.* **1995**, *328*, 248.
(16) Solymosi, F.; Berko, A.; Toth, Z. *Surf. Sci.* **1993**, *285*, 197.
(17) Rebholz, M.; Kruse, N. *J. Chem. Phys.* **1991**, *95*, 7745.
(18) Kruse, N.; Rebholz, M.; Matolin, V.; Chuah, G. K.; Block, J. H. *Surf. Sci.* **1991**, *238*, L457.
(19) Levis, R. J.; Jiang, Z. C.; Winograd, N. *J. Am. Chem. Soc.* **1988**, *110*, 4431; **1989**, *111*, 4605.

(20) Suwa, Y.; Ito, S.-I.; Kameoka, S.; Tomishige, K.; Kunimori, K. *Appl. Catal., A* **2004**, *267*, 9.
(21) Zambelli, T.; Wintterlin, J.; Trost, J.; Ertl, G. *Science* **1996**, *273*, 1688.
(22) Dahl, S.; Logadóttir, 'A.; Egeberg, R. C.; Larsen, J. H.; Chorkendorff, I.; Törnqvist, E.; Nørskov, J. K. *Phys. Rev. Lett.* **1999**, *83*, 1814.
(23) Greeley, J.; Nørskov, J. K.; Mavrikakis, M. *Annu. Rev. Phys. Chem.* **2002**, *53*, 319.
(24) Somorjai, G. A. *Introduction to Surface Chemistry and Catalysis*; Wiley: New York, 1994; pp 52, 88.
(25) Blöchl, P. E. *Phys. Rev. B: Condens. Matter Mater. Phys.* **1994**, *50*, 17953.
(26) Kresse, G.; Joubert, D. *Phys. Rev. B: Condens. Matter Mater. Phys.* **1999**, *59*, 1758.
(27) Kresse, G.; Furthmüller, J. *Phys. Rev. B: Condens. Matter Mater. Phys.* **1996**, *54*, 11169.
(28) Kresse, G.; Hafner, J. *Phys. Rev. B: Condens. Matter Mater. Phys.* **1993**, *47*, 558.
(29) Kresse, G.; Furthmüller, J. *Comput. Mater. Sci.* **1999**, *6*, 15.
(30) Perdew, J. P.; Wang, Y. *Phys. Rev. B: Condens. Matter Mater. Phys.* **1992**, *45*, 13244.
(31) Monkhorst, H. J.; Pack, J. D. *Phys. Rev. B: Condens. Matter Mater. Phys.* **1976**, *13*, 5188.
(32) Methfessel, M.; Paxton, A. T. *Phys. Rev. B: Condens. Matter Mater. Phys.* **1989**, *40*, 3616.
(33) Mills, G.; Jónsson, H.; Schenter, G. K. *Surf. Sci.* **1995**, *324*, 305.
(34) Wynne-Jones, W. F. K.; Eyring, H. *J. Chem. Phys.* **1935**, *3*, 492.
(35) Hill, T. L. *An Introduction to Statistical Thermodynamics*; Dover: New York, 1986.
(36) Hammer, B. *Surf. Sci.* **2000**, *459*, 323.
(37) Alavi, A.; Hu, P. J.; Deutsch, T.; Silverstrelli, P. L.; Hutter, J. *Phys. Rev. Lett.* **1998**, *80*, 3650.